Appl Phys B (2010) 99: 391–395
DOI 10.1007/s00340-010-4037-3

Applied Physics B
Lasers and Optics

RAPID COMMUNICATION

Multiwavelength fiber laser based on a photonic crystal fiber loop mirror with cooperative Rayleigh scattering

A.M.R. Pinto · O. Frazão · J.L. Santos · M. Lopez-Amo

Received: 9 December 2009 / Revised version: 29 March 2010 / Published online: 22 April 2010

Abstract In this work, a multiwavelength fiber Raman laser based on a highly birefringent photonic crystal fiber loop mirror is presented. A laser resonator is formed when the Raman amplification with cooperative Rayleigh scattering in a dispersion-compensating fiber is used as a distributed mirror and combined with a photonic crystal fiber loop mirror filtering structure. Stable multiwavelength lasing at room temperature is achieved due to the low temperature sensitivity of the highly birefringent photonic crystal fiber.

1 Introduction

Multiwavelength fiber lasers have been widely investigated in view of the demand of larger signal transmission capacity in optical fiber communication systems. This kind of fiber laser is very useful for applications such as dense wavelength division multiplexed systems, spectroscopy, optical fiber sensors, optical instrument testing, etc. Several flexible techniques to realize multiwavelength fiber lasers have been demonstrated, such as: making use of a semiconductor optical amplifier in a ring structure based in a fiber loop mirror (FLM) [1] or in a dual-pass Mach–Zehnder interferometer filter [2]; using ring resonators combined with fiber Bragg gratings (FBGs) and Raman amplification [3, 4]; by the integration of a fiber loop mirror with erbium-doped fibers (EDFs) [5]; via two fiber loop mirrors [6] or a highly birefringent (Hi-Bi) photonic crystal fiber (PCF) loop mirror [7]. The use of Hi-Bi PCFs in fiber loop mirrors leads to filters that have residual sensitivity to temperature variations when compared to conventional polarization maintaining fiber (PMF) based ones, leading to an improved stability of multiwavelength fiber lasers based on such filters [8–10].

Multiwavelength fiber lasers based on hybrid-gain configurations have been widely studied in recent decades. The hybrid-gain technique, which integrates Brillouin and erbium gains, has been reported to produce multiple wavelengths [11] by the use of a reverse S-shaped configuration with erbium-doped fibers and a Brillouin laser. Another hybrid-gain technique uses a Brillouin–Raman laser cavity with cooperative Rayleigh scattering. An example of this technique is the one performed using a high-power ytterbium fiber laser, an aluminum-coated mirror and a dispersion-compensating fiber (DCF) [12]. In this case it is demonstrated that the cooperative Rayleigh scattering with the Raman amplification can be used as a distributed mirror in the cavity to improve the generation of Brillouin Stokes combs [13]. Recently, a Raman fiber Bragg grating laser sensor with cooperative Rayleigh scattering was demonstrated for strain–temperature discrimination [14].

In this letter, the authors present a Hi-Bi PCF loop mirror filtering structure combined with a distributed mirror created by Raman amplification with cooperative Rayleigh scattering to demonstrate, at room temperature, a stable multiwavelength fiber laser.

A.M.R. Pinto (✉) · M. Lopez-Amo
Departamento de Ingeniería Eléctrica y Electrónica,
Universidad Pública de Navarra, Campus de Arrosadía,
31006 Pamplona, Navarra, Spain
e-mail: anamargarida.rodriguez@unavarra.es

O. Frazão · J.L. Santos
INESC Porto (Instituto de Engenharia de Sistemas
e Computadores do Porto), Departamento de Física,
Faculdade de Ciências, Universidade do Porto,
Rua do Campo Alegre, 687, 4169-007 Porto, Portugal

2 Experimental setup and results

The schematic configuration of the proposed multiwavelength Raman fiber laser is shown in Fig. 1. This experimental setup consists of a high-pump Raman laser at 1450 nm (maximum power of 5 W), a fiber loop mirror, two wavelength-division multiplexers (WDMs) (1450/1550 nm) and 1 km of dispersion-compensating fiber. The DCF presents a dispersion of -1041 ps nm^{-1} km^{-1}. The FLM is formed by a 3 dB optical coupler with low insertion loss, an optical polarization controller (PC) and 3.9 m of Hi-Bi PCF. The Hi-Bi PCF was spliced at both ends to single-mode fiber, the splices having a maximum loss of 2 dB each. This Hi-Bi PCF (Thorlabs PM-1550-01) is a polarization-maintaining PCF containing two large holes, operating at 1550 nm with a beat length of 4 mm and an attenuation of 1.0 dB/km (photograph in inset of Fig. 1). The diameters of the Hi-Bi PCF holes are 4.5 and 2.2 μm for the two big central holes and for the smaller ones, respectively. The pitch (spacing between the centers of two adjacent holes) of this PCF is 4.4 μm, the diameter of the holey region is 40 μm, while the outer diameter is 125 μm. The great advantage of using Hi-Bi PCF in this configuration is its temperature residual sensitivity (0.29 pm/°C) [15]. An optical spectrum analyzer (OSA) with a maximum resolution of 10 pm was used to observe the multiwavelength laser peaks.

Using the configuration proposed in Fig. 1, a multiwavelength linear cavity can be achieved. The cavity resonator is created by the combination of a fiber loop mirror and a distributed mirror. The distributed mirror is created by Rayleigh scattering and double Rayleigh scattering formed in the DCF as a result of the injected Raman amplification.

In the Hi-Bi PCF fiber loop mirror an optical coupler splits the input signal equally into two counter-propagating waves which subsequently recombine (at the coupler) after propagating around the loop mirror. A variable interference term in the output port can be obtained when a section of Hi-Bi PCF is located inside the loop mirror. Figure 2 shows the spectral filter transfer function associated with the Hi-Bi PCF loop mirror. In this case, the spacing between two consecutive peaks of the filter is ≈0.8 nm (100 GHz). This spectral spacing can be easily adjusted by simply changing the length of the Hi-Bi PCF.

The distributed mirror is an outcome of large Raman gain. When the Raman gain is very high, not only Rayleigh scattering is generated by the pump signal, but this Rayleigh scattering will also generate a double Rayleigh scattering signal. This double Rayleigh scattering signal, combined with the amplified spontaneous emission of the Raman amplifier, induces incoherent multiple path interference, which is noise associated with the beating of multiple different delayed replicas of the signal itself. The distributed mirror has a similar effect as two discrete reflectors with effective reflectances proportional to the ratios of total backscattered to incident power [16].

For better understanding of the distributed mirror, the effects of Raman pump power combined with Rayleigh scattering and the pumping direction were analyzed. In order to perform this analysis, the OSA was located in such a way as to observe two different situations: one being the use of a counter-propagating pump and the other of a co-propagating pump. Figure 3a presents the Rayleigh distributed lasing created by the counter-propagating Raman pump. Figure 3b shows double Rayleigh lasing obtained in the output laser cavity (co-propagating Raman pump). Comparing the two graphics, it can be seen that the Rayleigh lasing has much higher intensity than that of the double Rayleigh lasing.

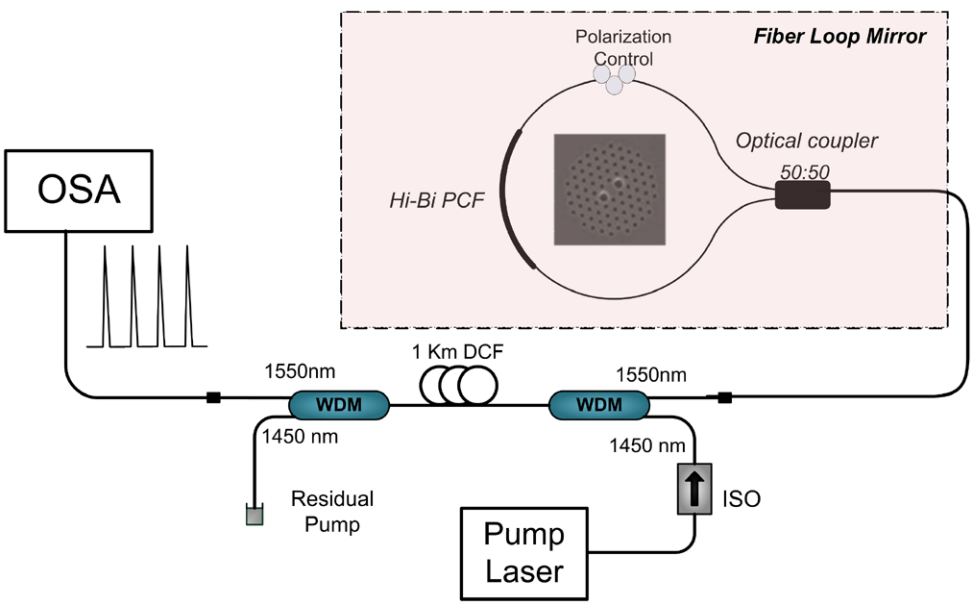

Fig. 1 Schematic diagram of the proposed configuration using the Hi-Bi PCF (*inset*: photograph of the Hi-Bi PCF)

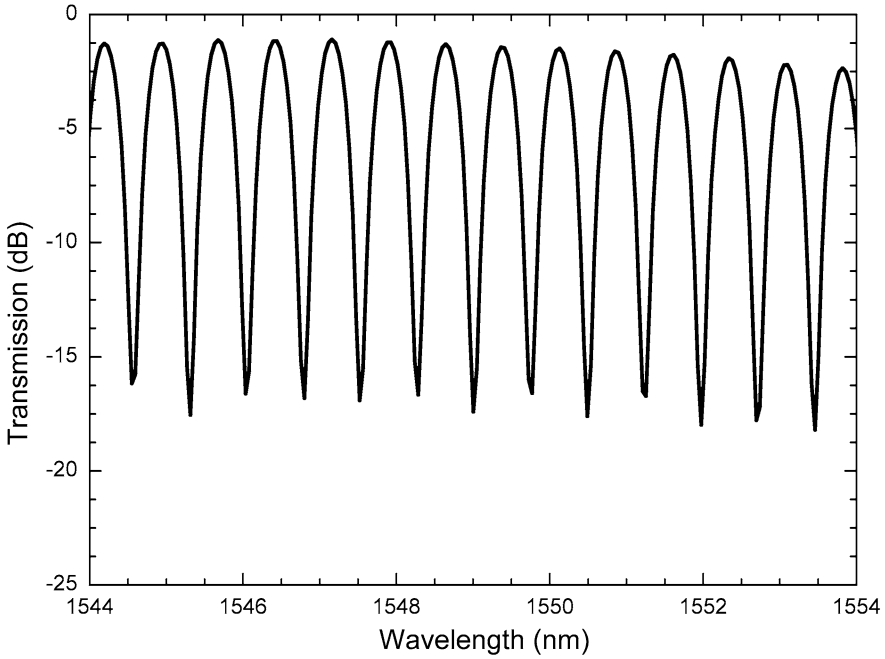

Fig. 2 Transmission spectral characteristic of the Hi-Bi PCF loop mirror

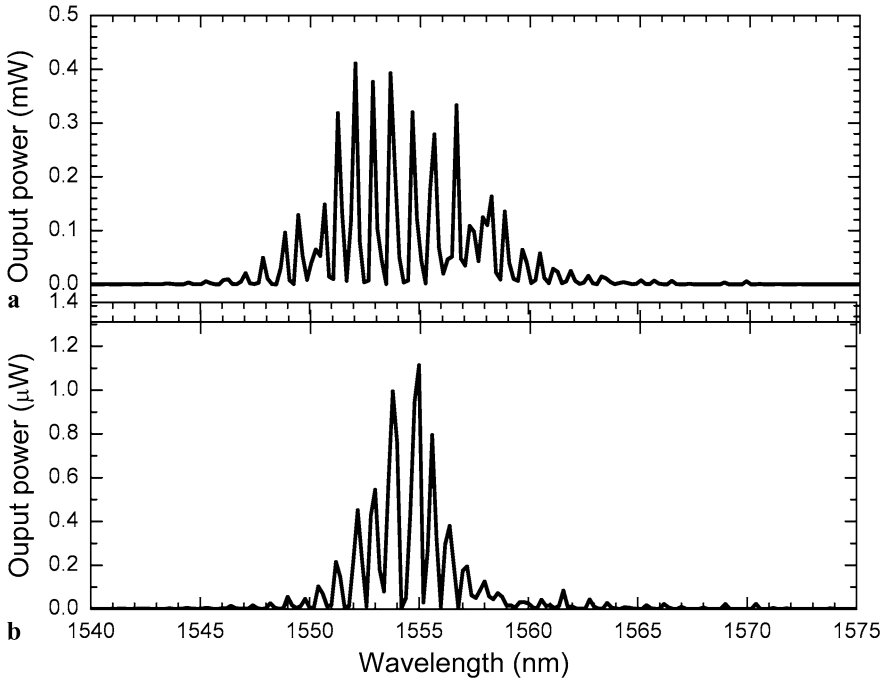

Fig. 3 Output spectra for (**a**) Rayleigh lasing and (**b**) double Rayleigh lasing

This is due to the high power injected in the DCF combined with the counter-propagating Raman pump. The use of a counter-propagating pump ensures maximum randomization of the polarization as well as near-zero temporal fluctuations, while the use of a co-propagating pump implies that the random fluctuations of the pump power are transferred to the amplified signal. As such, the use of a counter-propagating pump laser increases the lasing efficiency.

After the fiber loop mirror and the distributed mirror (using counter-propagating pump) had been characterized, they were spliced together as is shown in the schematic diagram of the proposed fiber laser. Figure 4 presents the spectral response of the proposed fiber laser for two different pump powers after optimized adjustment of the polarization controller. There are 17 lasing channels. The number of lasing channels is limited by the Raman gain range and the length of the Hi-Bi PCF. Since the Raman gain is always the same (keeping the same length of DCF), by simply changing the length of the Hi-Bi PCF one can insert more or fewer channels. Making use of the equation $\Delta\lambda = \lambda^2/\beta L$, where $\Delta\lambda$ is

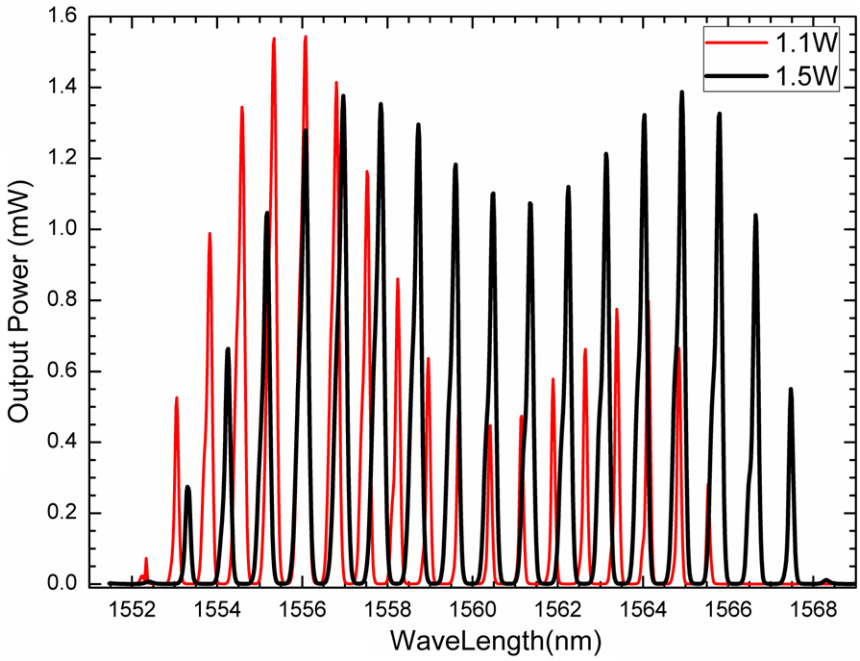

Fig. 4 Spectral response of the fiber laser for two different pump powers

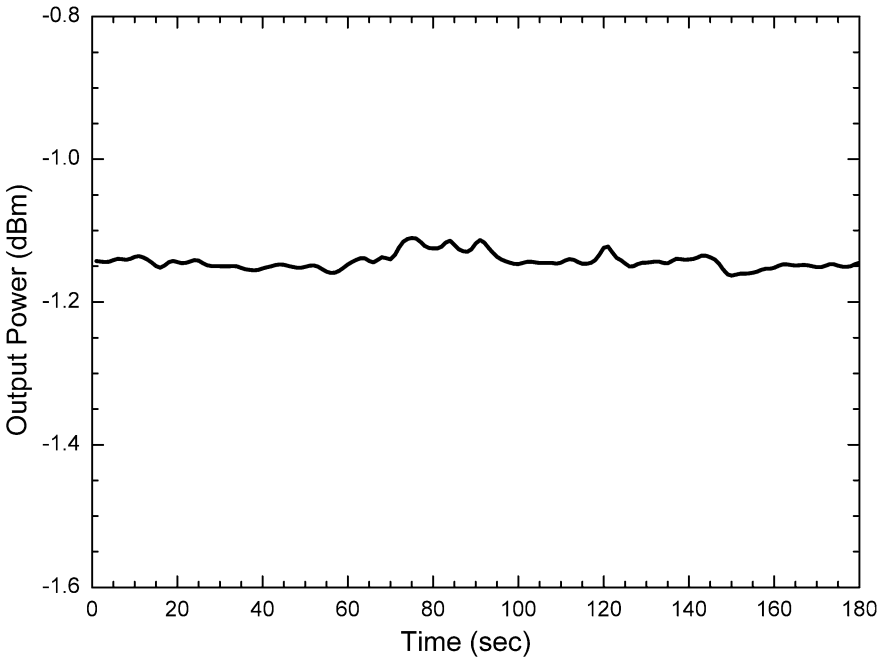

Fig. 5 Power fluctuation of an emission line of the proposed fiber laser

the peak to peak distance between two consecutive channels, λ is the wavelength, L is the length of the Hi-Bi PCF in the FLM and β is the birefringence of the Hi-Bi PCF, one can notice that the spacing between channels is inversely proportional to the length of the Hi-Bi PCF. As such, if the length of the Hi-Bi PCF is enlarged the spacing between channels will diminish, resulting in that in the same range of wavelengths there will be more channels. Therefore, the lasing spectrum can be tailored by changing the length of the Hi-Bi PCF.

Also, in Fig. 4, it can be observed that the output power increases when the pump power rises. This is due to the Raman amplification, since the Raman gain in the selected range is directly proportional to the pump power. The non-flat-amplitude bandwidth is also determined by the choice of the Raman pump wavelength. To solve this problem, it is necessary to use two distinct Raman pump wavelengths for a flat optimization of the amplitude bandwidth.

Stability measurements were made in order to determine the power fluctuations of the multiwavelength fiber Raman

laser channels. It was observed that from the 17 lasing channels only the middle 15 were stable. Figure 5 shows the optical power fluctuation of the proposed multiwavelength Raman fiber laser for a selected emission line. This peak was isolated using an optical filter at 1560 nm. The line width of this peak was found to be ∼300 pm, the peak power was ~ -1.14 dBm and the signal-to-noise ratio (SNR) was larger than 30 dB. As can be observed, these fluctuations do not exceed 0.05 dBm in a time window of some minutes. For all 15 channels the power fluctuations are very small, as expected since the FLM has poor sensitivity to environmental noise and the Raman laser is stable at room temperature.

3 Conclusions

A multiwavelength fiber Raman laser based on a highly birefringent photonic crystal fiber loop mirror was proposed and demonstrated. The Hi-Bi PCF loop mirror is used as a filter and is combined with a distributed mirror to produce a laser resonator. This distributed mirror is the result of the double scattering produced in the DCF by the Raman amplification. Stable multiwavelength lasing was achieved for 15 channels. The number of lasing channels can be easily tuned by changing the length of the Hi-Bi PCF employed in the FLM. Even more, a wider wavelength range can be achieved in the linear cavity resonator if additional Raman pumps are added to the proposed setup. Furthermore, by simply changing the pump power of these additional Raman pumps it is possible to equalize the peak powers of the obtained laser. The proposed multiwavelength Raman fiber laser may be utilized in telecommunications and in sensor systems.

Acknowledgement The authors are grateful to the Spanish Government project TEC2007-67987-C02-02 and the European COST Action 299.

References

1. D. Liu, N.Q. Ngo, H. Liu, D. Liu, Opt. Commun. **282**, 1598 (2009)
2. F. Wang, X. Zhang, Y. Yu, X. Huang, Opt. Laser Technol. **42**, 285 (2010)
3. Y. Liu, D. Liu, H. Wang, Microw. Opt. Technol. Lett. **50**, 3053 (2008)
4. S. Diaz, M. Lopez-Amo, J. Opt. Commun. **27**, 296 (2006)
5. D.M. Liang, X.F. Xu, Y. Li, J.H. Pei, Y. Jiang, Z.H. Kang, J.Y. Gao, Laser Phys. Lett. **4**, 57 (2006)
6. D. Chen, Laser Phys. Lett. **4**, 437 (2007)
7. C.S. Kim, R.M. Sova, J.U. Kang, Opt. Commun. **218**, 291 (2003)
8. D.H. Kim, J.U. Kang, Opt. Express **12**, 4490 (2004)
9. Z.Y. Liu, Y.G. Liu, J.B. Du, G.Y. Ka, X.Y. Dong, Laser Phys. Lett. **5**, 446 (2008)
10. C. Daru, S. Qin, L. Shen, H. Chi, S. He, Microw. Opt. Technol. Lett. **48**, 2416 (2006)
11. G.J. Cowle, D.Y. Stepanov, IEEE Photonics Technol. Lett. **8**, 1465 (1996)
12. B. Min, P. Kim, N. Park, IEEE Photonics Technol. Lett. **13**, 1352 (2001)
13. A.K. Zamzuri, M.I. Md Ali, A. Ahmad, R. Mohamad, M.A. Mahdi, Opt. Lett. **31**, 918 (2006)
14. O. Frazão, C. Correia, J.M. Baptista, J.L. Santos, Meas. Sci. Technol. **20**, 45203 (2009)
15. C. Zhao, X. Yang, C. Lu, W. Jin, M.S. Demokan, IEEE Photonics Technol. Lett. **16**, 2535 (2004)
16. J.L. Gimlett, M.Z. Iqbal, N.K. Cheung, A. Righetti, F. Fontana, G. Grass, IEEE Photonics Technol. Lett. **2**, 211 (1990)